Increasing the Hydrophilicity of Cyclic Ketene Acetals Improves the Hydrolytic Degradation of Vinyl Copolymers and the Interaction of Glycopolymer Nanoparticles with Lectins

Théo Pesenti, Emilie Gillon, Seika Ishii, Samir Messaoudi, Yohann Guillaneuf, Anne Imberty, Julien Nicolas

Increasing the Hydrophilicity of Cyclic Ketene Acetals Improves the Hydrolytic Degradation of Vinyl Copolymers and the Interaction of Glycopolymer Nanoparticles with Lectins

*Théo Pesenti,[1] Emilie Gillon,[2] Seika Ishii,[1] Samir Messaoudi,[3] Yohann Guillaneuf,[4] Anne Imberty,[2] Julien Nicolas[1,]**

[1] Université Paris-Saclay, CNRS, Institut Galien Paris-Saclay, 91400 Orsay, France

[2] Université Grenoble Alpes, CNRS, CERMAV, 38000 Grenoble, France

[3] Université Paris-Saclay, CNRS, BioCIS, 91400 Orsay, France

[4] Aix-Marseille-Univ., CNRS, Institut de Chimie Radicalaire, UMR 7273, 13397 Marseille, France

*To whom correspondence should be addressed.

Email: julien.nicolas@universite-paris-saclay.fr

Tel.: +33 1 80 00 60 81

Abstract

Radical ring-opening polymerization (rROP) of cyclic ketene acetals (CKAs) with traditional vinyl monomers allows the synthesis of degradable vinyl copolymers. However, since the most commonly used CKAs are hydrophobic, most degradable vinyl copolymers reported so far degrade very slowly by hydrolysis under physiological conditions (phosphate buffer saline, pH 7.4, 37°C) which could be detrimental for biomedical applications. Herein, to design advanced vinyl copolymers by rROP with high CKA content and enhanced degradation profiles, we reported the copolymerization of 2-methylene-1,3,6-trioxocane (MTC) as a CKA with vinyl ether (VE) or maleimide (MI) derivatives. By performing a point-by-point comparison between the MTC/VE and MTC/MI copolymerization systems, and their counterparts based on 2-methylene-1,3-dioxepane (MDO) and 5,6-benzo-2-methylene-1,3-dioxepane (BMDO), we showed negligible impact on the macromolecular characteristics and similar reactivity ratios, suggesting successful substitution of MDO and BMDO by MTC. Interestingly, owing to the hydrophilicity of MTC, the obtained copolymers exhibited a faster hydrolytic degradation under both accelerated and physiological conditions. We then prepared MTC-based glycopolymers which were formulated into surfactant-free nanoparticles, exhibiting excellent colloidal stability up to 4 months and complete degradation under enzymatic conditions. Importantly, MTC-based glyconanoparticles also showed a similar cytocompatibility toward two healthy cell lines and a much stronger lectin affinity than MDO-based glyconanoparticles.

1. Introduction

Polymers are a major class of materials with many possible applications (e.g., packaging, construction, coatings/paints, automotive, electronics, medicine, agriculture, etc.).[1-4] As a component of plastics, they have known a steady increase in global production, reaching 368 million tons in 2019. The most representative vinyl polymers (polypropylene, polyethylene and polyvinylchloride) account for more than 50 % of the polymers used. However, plastic pollution has become a major concern in recent years in terms of environmental and public health issues. Although the share of recycled plastics has increased over the past 15 years, around 25 % of plastics were landfilled in 2018. As a result, these polymers accumulate in the environment due to the lack of cleavable bonds in their backbone, which prevents their (bio)degradation.[5]

The non-degradability of vinyl polymers also raises questions about their application in the biomedical field. For instance, non-degradable polymer-based implants have to be surgically removed after use which is rather invasive and can have consequences for patients.[6-8] They are also more prone to bacterial infections than their biodegradable counterparts.[7] Polymer-based nanoscale systems also represent a significant part of nanomedicine research.[8-9] Non-degradable polymers can be excreted from the body by renal elimination if their average molar mass is below the glomerular threshold (typically ~30–45 kDa, depending on the polymer structure).[10] Yet, elimination of polymers from the body is a complex mechanism which depends on other parameters such as the polymer size and shape, and different metabolization mechanisms.[10] Moreover, polymers are composed of a distribution of polymer chains of different molar masses. Consequently, the elimination process can differ from one polymer chain to another.[11] Therefore, there is some concern about the potential toxicity associated with their (partial) accumulation after their use.[10, 12]

In this context, the development of (bio)degradable vinyl polymers to compete with traditional aliphatic polyesters obtained by ring-opening polymerization (ROP),[13] such as polycaprolactone (PCL), poly(D,L-lactide) (PLA) and poly(D,L-lactide-*co*-glycolide) (PLGA), is

receiving much attention.[14] Despite some important limitations (e.g., rather limited structural and architectural diversity, not straightforward functionalization), aliphatic polyesters are still considered the gold standards in the field. However, recent years have seen the development of alternative synthetic routes to produce (bio)degradable polymers,[14] and in particular the resurgence of radical ring-opening polymerization (rROP) of cyclic ketene acetals (CKA).[15-17] In the past few years, rROP has indeed benefited from the advantages of modern polymerization techniques such as reversible deactivation radical polymerization (RDRP),[18] and from the discovery of new copolymerization systems made possible by the broad diversity of common vinyl monomers. This allowed the synthesis of (well-defined) degradable vinyl polymer architectures with advanced properties and functionalities under less stringent polymerization conditions than those of ROP-derived aliphatic polyesters.

CKAs can copolymerize with many common vinyl monomers, such as (meth)acrylates, vinyl acetates, acrylamides and, more recently, maleimides (MIs) and vinyl ethers (VEs).[15-16] Favorable reactivity ratios with MIs and VEs allowed the synthesis of degradable copolymers containing ~50 mol %[19-21] and ~90 mol % CKA units, respectively,[22-23] thus opening the door to functional, polyester-like copolymers by a radical mechanism. This is in contrast to copolymerization with (meth)acrylates which typically does not exceed ~25 mol % CKA units, and yields rather segmentable vinyl copolymers.[15] Having high CKA content copolymers can lead to materials that mimic traditional polyesters in terms of properties and degradability, while the versatility of radical polymerization may allow their facile functionalization via the use of functional initiators/controlling agents and/or functional MI and VE moieties. However, the number of CKAs that can effectively copolymerize with vinyl monomers is still quite limited. Among them, 2-methylene-1,3-dioxepane (MDO), 5,6-benzo-2-methylene-1,3-dioxepane (BMDO) and 2-methylene-4-phenyl-1,3-dioxolane (MPDL) are by far the most used.[15-16] Moreover, they are all hydrophobic, which may restrain their applications where water solubility/hydrophilicity is a key parameter and when fast hydrolytic/enzymatic degradation is required. For instance, hydrolytic degradation under

physiological conditions (phosphate buffer saline, pH 7.4, 37°C) of hydrophobic copolymers containing ~25–90 mol % of these hydrophobic CKAs has been shown to occur on a time scale of several months to a year, depending on the copolymer composition.[23-24] Also, the use of aromatic ring-containing CKAs, such as MPDL or BMDO, has also been shown to prevent efficient enzymatic degradation of the copolymers,[24] likely because of high steric hindrance and hydrophobicity in the vicinity of the ester group, preventing efficient solvation and enzyme access. Although this can be compensated for by selecting hydrophilic vinyl monomers,[24-25] a simpler strategy would be to use hydrophilic CKAs. This would also allow the main vinyl monomer to be dedicated to other purposes, for example as a handle to introduce functional groups. Unfortunately, the synthesis of hydrophilic CKAs or heteroatom-bearing CKAs is very challenging.[26]

2-Methylene-1,3,6-trioxocane (MTC) is one of the very few heteroatom-bearing CKAs that has been reported.[27-29] Yet it has received much less attention than MDO, BMDO and MPDL.[15] Most of the studies on MTC were published more than 15 years ago and focused on its free-radical copolymerization with various vinyl monomers such as styrene,[30] vinyl acetate,[30] methyl vinyl ketone,[31] *N*-vinyl-2-pyrrolidone (NVP),[32] *N*-isopropyl acrylamide,[33] maleic anhydride[34] and divinylapidate.[35-36] While PMTC can be biodegraded by microorganisms in soils but hardly degrades in phosphate buffer saline (PBS),[37] MTC-based copolymers were enzymatically degraded by esterases.[29] More recently, P(MTC-*co*-MDO) copolymers were prepared,[38] while MTC was successfully copolymerized with gaseous ethylene by cobalt-mediated radical copolymerization[39] and reversible addition-fragmentation chain transfer (RAFT)[40] to yield degradable copolymers. Also, semi-batch copolymerization of MTC and NVP was reported to achieve linear copolymers with uniform insertion of ester groups along the chain.[41]

Herein, to tackle the very slow hydrolytic degradations of MDO-, BMDO- and MPDL-containing copolymers, we sought to substitute these CKAs by MTC to take advantage of its

hydrophilic properties due to its oligo(ethylene glycol)-like structure once opened. We applied this methodology to P(CKA-*co*-MI) and P(CKA-*co*-VE) copolymers, which represent two of the most promising rROP copolymerization systems ever developed in terms of CKA content and functionalization possibilities.[15] We synthesized a substantial library of MTC-containing copolymers (Figure 1) and performed point-by-point comparisons with their counterparts based on common hydrophobic CKAs, on the basis of their macromolecular characteristics, reactivity ratios and hydrolytic degradation. Overall, we showed that MTC can successfully replace more hydrophobic CKAs with minimal impact on the macromolecular characteristics of the resulting copolymers and, more importantly, can induce significantly faster hydrolytic degradation kinetics under physiological conditions. To further demonstrate the added value of MTC, we also showed that degradable galactose (Gal)-based P(MTC-*co*-GalVE) glycopolymer nanoparticles exhibited significantly enhanced interaction with LecA, a tetrameric β-galactose-binding lectin from the *Pseudomonas aeruginosa* bacterium,[42-43] conversely to P(MDO-*co*-GalVE) glycopolymer nanoparticles, which gave non-specific interactions.[44] The P(MTC-*co*-GalVE) nanoparticles also exhibited excellent cytocompatibility on two representative healthy cell lines.

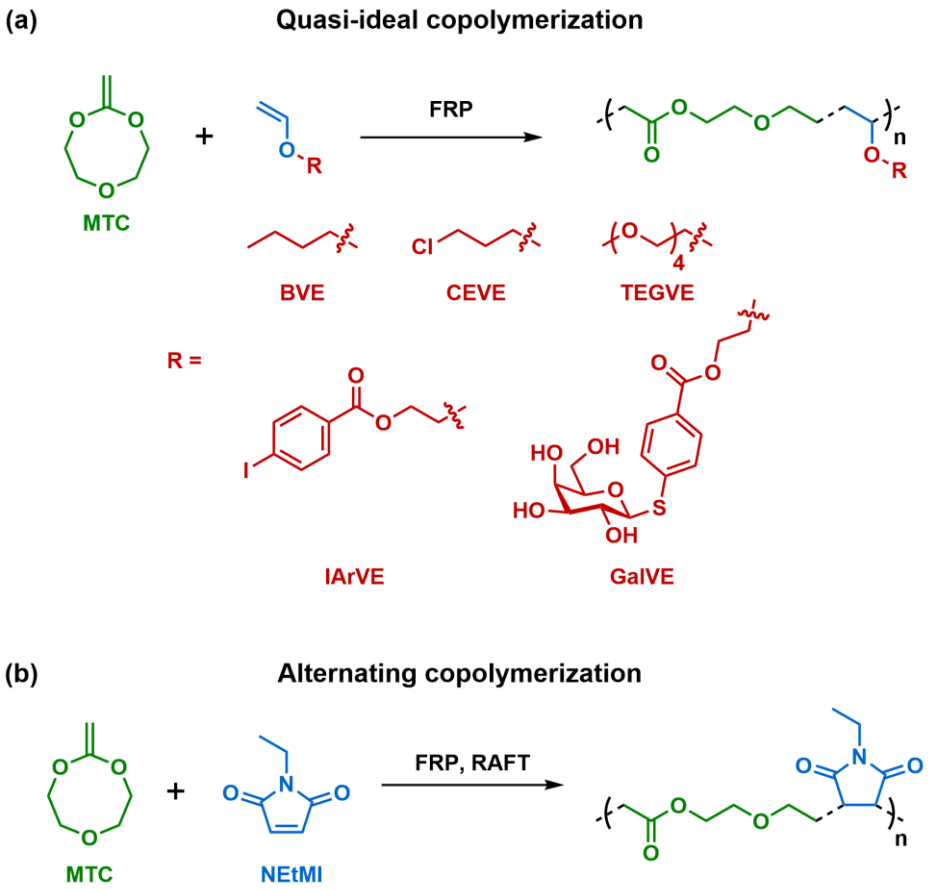

Figure 1. (a) Free-radical polymerization (FRP) of 2-methylene-1,3,6-trioxocane (MTC) with vinyl ether (VE) derivatives (BVE = *n*-butyl vinyl ether, CEVE = 2-chloroethyl vinyl ether, TEGVE = tetraethylene glycol methyl vinyl ether, IArVE = *p*-iodoaryl vinyl ether, GalVE = β-thiophenylgalactose vinyl ether). (b) FRP or reversible addition fragmentation chain transfer (RAFT) polymerization of MTC and *N*-ethylmaleimide (NEtMI).

2. Experimental part

2.1. Materials

Azobisisobutyronitrile (AIBN, 98 %, purchased from Sigma-Aldrich) was recrystallized from methanol (MeOH). Tetraethylene glycol methyl vinyl ether (TEGVE, Sigma-Aldrich) was purified by column chromatography on silica gel (cyclohexane:EtOAc 100:0 to 80:20 v/v). Dodecylsulfanylthiocarbonylsulfanyl-2-methylpropionic acid (DDMAT, 98 %) was obtained from Sigma-Aldrich and used as received. Lipase B *Candida antarctica* immobilized on Immunobead 150, recombinant from yeast (4584 U/g) was purchased from Sigma-Aldrich. LecA was produced recombinantly in *E. coli* and purified as previously described.[45] All other

reagents were purchased from Merck, TCI Chemicals or Thermo Fisher Scientific and used as received. MDO and BMDO were prepared by adapting a previously published method, using the cyclic bromoacetal as intermediate.[22, 46] Iodinated and β-galactosylated vinyl ether derivatives were synthesized as previously described.[44] MDO- and BMDO-based copolymers were prepared as previously described.[20, 22-23] Diethylazobisisobutyrate (DEAB) was kindly supplied by Arkema. Deuterated solvents were purchased from Eurisotop. All other solvents were purchased from Carlo Erba at the highest grade.

2.2. Analytical methods

2.2.1. Nuclear Magnetic Resonance Spectroscopy (NMR)

NMR spectroscopy was performed in 5 mm diameter tubes in $CDCl_3$ at 25°C. ^{1}H and ^{13}C NMR spectroscopy was performed on a Bruker Avance spectrometer at 300 MHz. The chemical shifts are reported in ppm (δ units), and internal solvent signal (δ = 7.26 ppm for $CDCl_3$) was used as a reference. ^{1}H-^{13}C heteronuclear multiple bond correlation (HMBC) NMR experiments were performed on a Bruker Avance spectrometer at 400 MHz.

2.2.2. Size Exclusion Chromatography (SEC)

SEC analysis of copolymers (except P(MTC-*co*-GalVE) copolymers) was performed on a Tosoh EcoSEC HLC-8320 GPC with two columns from Agilent (PL-gel MIXED-D, 300 × 7.5 mm, beads diameter: 5 µm, linear part: 400–4 × 10^5 g.mol^{-1}). Analyses were performed at 35°C in $CHCl_3$ (HPLC grade) at a flow-rate of 1 mL.min^{-1}. Toluene (0.3 vol %) was used as flow-rate marker. Samples were filtered with a 0.22-µm PTFE filter before analysis. The calibration curve was based on poly(methyl methacrylate) (PMMA) standards (M_p = 1 850–1 916 000 g.mol^{-1}) from Agilent. The EcoSEC Analysis software enabled the determination of the number-average molar mass M_n, the weight-average molar mass M_w and the dispersity ($Đ = M_w/M_n$).

SEC analysis of P(MTC-*co*-GalVE) copolymers was performed on a Viscotek TDA/GPCmax from Malvern with two columns from Agilent (PL PolarGel-M, 300 × 7.5 mm,

bead diameter: 8 µm, linear part: 1 000–500 000 g.mol^{-1}). Analyses were performed at 60 °C in DMSO (HPLC grade) with 10 mM LiBr (filtered over 0.22-µm PTFE filters) at a flow rate of 0.7 mL.min^{-1}. 2,6-Di-*tert*-butyl-4-methylphenol (BHT) (0.3 wt %) was used as flow rate marker. Samples were filtered with a 0.22-µm PTFE filter before analysis. The calibration curve was based on PMMA standards (M_p = 540–342 900 g.mol^{-1}) from Agilent. The OmniSEC software enabled the determination of M_n, M_w and $Đ$.

SEC analysis of the degraded copolymers was performed at 30°C in $CHCl_3$ with trifluoroacetic acid (TFA, 0.1 vol %) as eluent on a system equipped with two columns from Agilent (PL-gel MIXED-D, 300 × 7.5 mm, beads diameter: 5 µm, linear part: 400–4 × 10^5 g.mol^{-1}), a differential refractive index detector (Spectrasystem RI-150 from Thermo Electron Corp.) and a Waters 515 HPLC Pump at a flow rate of 1 mL.min^{-1}. Toluene (0.3 vol %) was used as flow rate marker. Samples were filtered with a 0.22-µm PTFE filter before analysis. The calibration curve was based on PMMA standards (M_p = 540–342 900 g.mol^{-1}) from Agilent. The OmniSEC software enabled the determination of M_n, M_w and $Đ$.

2.2.3. Dynamic Light Scattering (DLS)

The intensity-average nanoparticle diameter (D_z) was measured by DLS with a Nano ZS from Malvern with a detector angle of 173° (back scattering) at 25 °C. Samples were diluted 1:9 in the appropriate aqueous medium prior to measurement (except for lectin interaction assays). Each measurement was performed in triplicate

2.2.4. ζ-potential measurement

ζ-potential was measured with a Nano ZS from Malvern at 25°C. samples were diluted 1:9 in NaCl 1 mM prior to measurement. Each measurement was performed in triplicate.

2.3. Synthesis procedures

2.3.1. Synthesis of 2-methylene-1,3,6-trioxocane (MTC)

The synthesis of MTC was adapted from previously described protocols.[38, 46] Bromoacetaldehyde dimethyl acetal (50 g, 296 mmol, 1 equiv.), diethylene glycol (31.4 g,

296 mmol, 1 equiv.) and *p*-toluenesulfonic acid monohydrate (0.17 g, 0.9 mmol, 0.003 equiv.) were heated to 130°C overnight in a 250-mL flask equipped with a distillation set-up. After removing the distilled methanol, the product was purified by distillation under reduced pressure (T_{bath} = 130 °C, T_{vapor} = 63 °C, P = 1 mbar). 2-(Bromomethyl)-1,3,6-trioxocane (Br-MTC) was obtained as a colorless liquid which crystallized at room temperature with 30 % yield (18.5 g, 88 mmol).

Br-MTC (10 g, 47 mmol, 1 equiv.), Aliquat 336 (0.38 g, 1 mmol, 0.02 equiv.) and anhydrous THF (20 mL) were mixed at 0°C under Argon atmosphere for 30 min. Potassium *tert*-butoxide (11.5 g, 94 mmol, 2 equiv.) was progressively added and the reaction was left at 0°C under Argon atmosphere for 2 h. Cold diethyl ether was added, and the insoluble salts were filtered off. Solvents were evaporated from the filtrate using a Rotavapor (P = 100 mbar, T = 35 °C). The product was purified by distillation under reduced pressure (T_{bath} = 125 °C, T_{vapor} = 59 °C, P = 20 mbar). MTC was obtained as a colorless liquid with 30 % yield (1.8 g, 14 mmol).

2.3.2. Synthesis of copolymers

Synthesis of poly(2-methylene-1,3,6-trioxocane-co-n-butyl vinyl ether) ***P(MTC-co-BVE).*** In a 7-mL vial, MTC (840 mg, 6.5 mmol), BVE (162 mg, 1.6 mmol) and DEAB (62 mg, 0.2 mmol) were introduced. The mixture was degassed by Argon bubbling under magnetic stirring at room temperature for 30 min. The mixture was immersed in a preheated oil bath at 70°C for 8 h. Unreacted monomers were removed by two consecutive precipitations in 60 mL of cold *n*-heptane. For each precipitation, the pellet was recovered, and the supernatant was centrifuged at 10 000 rpm for 10 min. All pellets were combined, then dried under high vacuum until constant weight. A colorless oil was obtained (506 mg). 2-3 Drops of bromobenzene were added to the crude as an internal reference to allow the determination of the BVE conversion (which was used for the determination of reactivity ratios using the Skeist equation).

Synthesis of poly(2-methylene-1,3,6-trioxocane-co-tetra(ethylene glycol) methyl vinyl ether) ***P(MTC-co-TEGVE)****.* The same protocol as for the synthesis of **P(MTC-*co*-BVE)** was followed by replacing BVE by TEGVE with the following amounts: MTC (356 mg, 2.7 mmol), TEGVE (148 mg, 0.6 mmol) and DEAB (27 mg, 0.1 mmol). A colorless oil was obtained (126 mg).

Synthesis of poly(2-methylene-1,3,6-trioxocane-co-2-chloroethyl vinyl ether) ***P(MTC-co-CEVE).*** The same protocol as for **P(MTC-*co*-BVE)** was followed by replacing BVE by CEVE with the following amounts: MTC (415 mg, 3.2 mmol), CEVE (84 mg, 0.8 mmol) and DEAB (31 mg, 0.1 mmol). A colorless oil was obtained (141 mg).

Synthesis of poly(2-methylene-1,3,6-trioxocane-co-para-iodoaryl vinyl ether) ***P(MTC-co-IArVE).*** We adapted our previously reported protocol[44] by replacing MDO by MTC with the following amounts: MTC (451 mg, 3.5 mmol), IArVE (60 mg, 0.2 mmol) and DEAB (20 mg, 0.1 mmol). A colorless viscous solid was obtained (144 mg).

Synthesis of poly(2-methylene-1,3,6-trioxocane-co-β-thiophenylgalactose vinyl ether) ***P(MTC-co-GalVE).*** A peracetylated **P(MTC-*co*-(AcO)$_4$GalVE)** copolymer was synthesized according to our previously reported protocol[44] by replacing MDO by MTC with the following amounts: MTC (1.191 g, 9.2 mmol), (AcO)$_4$GalVE (268 mg, 0.5 mmol) and DEAB (50 mg, 0.2 mmol). Purification of the copolymer was performed by 4 consecutive precipitation in 75 mL of MeOH:H_2O (9:1 v/v) previously cooled down by an ice bath of aqueous NaCl. A yellowish oil was obtained (231 mg). Deprotection was performed as previously described with the following amounts: **P(MTC-*co*-(AcO)$_4$GalVE)** (200 mg), hydrazine monohydrate (60 µL) and dry THF (9 mL). A yellowish oil was obtained (136 mg).

Synthesis of poly(2-methylene-1,3,6-trioxocane-co-N-ethylmaleimide) ***P(MTC-co-NEtMI)*** *by free radical copolymerization.* In a 14-mL vial (vial A), NEtMI (147 mg, 1.2 mmol) and AIBN (8 mg, 0.05 mmol) were solubilized in 2.35 mL of anhydrous toluene. In another 14-mL vial (vial B), MTC (157 mg, 1.2 mmol) was diluted in 2.35 mL of anhydrous toluene. Both mixtures were degassed by Argon bubbling for 30 min. With an Argon-purged syringe, vial B was transferred into vial A. Vial A was immersed in a preheated oil bath at 85°C for 6

h. Unreacted monomers were purified by 2 precipitations in 50 mL of cold diethyl ether. For each precipitation, the pellet was recovered, and the supernatant was centrifuged at 10 000 rpm for 10 min. All pellets were combined then dried under high vacuum until constant weight.

For the determination of reactivity ratios, the copolymerization time was reduced to 7 min to ensure a monomer conversion below 20 %. For purification of unreacted monomers, the crude was concentrated under reduced pressure and precipitated twice in cold diethyl ether as described above.

Synthesis of poly(2-methylene-1,3,6-trioxocane-co-N-ethylmaleimide) ***P(MTC-co-NEtMI)*** *by RAFT polymerization.* In a 14-mL vial (vial A), NEtMI (128 mg, 1.0 mmol), AIBN (0.4 mg, 2 µmol) and RAFT agent (8 mg, 0.02 mmol) were solubilized in 2.3 mL of anhydrous toluene. The mixture was degassed by Argon bubbling for 30 min. In another 14-mL vial (vial B), MTC (150 mg, 1.2 mmol) was diluted in 2.3 mL of anhydrous toluene. The mixture was degassed by Argon bubbling for 30 min. With an Argon-purged syringe, vial B was transferred into vial A. Vial A was immersed in a preheated oil bath at 85°C. The crude was sampled with Argon-purged syringe at different times.

2.4. Degradation procedures

2.4.1. Degradation under accelerated conditions

In a 7-mL vial, 50 mg of copolymer was solubilized in 2.5 mL of THF. After solubilization, 2.5 mL of sodium hydroxide (NaOH, 0.1 wt %) in methanol was added. The mixture was stirred at room temperature. Samples (1 mL) were periodically withdrawn and immediately dried under high vacuum. 2 mL of $CHCl_3$ and 1 mL of aqueous HCl 1 M were added. After vortexing, the top aqueous layer was discarded, and the bottom organic layer was washed two more times with aqueous HCl 1 M. Solvent was then evaporated under reduced pressure. The degradation products were analyzed by SEC in $CHCl_3$ (TFA 0.1 vol %, PMMA calibration).

2.4.2. Hydrolytic degradation under physiological conditions

In a 7-mL vial containing 20 mg of copolymer, 2 mL of PBS (0.1 M, pH 7.4) was added. The vial was vortexed for 10 s, then mechanically stirred in an orbital sharker (37 °C, 125 rpm). At a given time point, the vial was withdrawn from the shaker, and the mixture was freeze-dried. 2 mL of $CHCl_3$ was added. After being vortexed, the resulting mixture was filtered over 0.22-µm hydrophobic PTFE filters to remove salt. The degradation products were analyzed by SEC in $CHCl_3$ (TFA 0.1 vol %, PMMA calibration).

2.4.3. Enzymatic degradation

In a 20-mL vial, 2 mL of **P(MTC-*co*-GalVE)** nanoparticle suspension (5 $mg.mL^{-1}$) were diluted with 2 mL of PBS (25 mM, pH 7.2). 87 mg of Lipase B from *Candida antarctica* (4584 $U.g^{-1}$) was then added to obtain 100 $U.mL^{-1}$. After incubation at 37 °C (1 h, 125-rpm orbital shaking), the reaction medium was freeze-dried and then solubilized in $CHCl_3$/TFA (0.1 vol %). Enzymes and salts were removed by filtration over a 0.22-µm hydrophobic PTFE filter. $CHCl_3$ was evaporated under reduced pressure and the degradation products were analyzed by SEC in $CHCl_3$ (TFA 0.1 vol %, PMMA calibration).

2.5. Isothermal titration calorimetry (ITC)

Recombinant lyophilized LecA was dissolved in water in the presence of 100 µM $CaCl_2$ and degassed. The LecA concentration was determined by measuring the optical density (Nanodrop) by using a theoretical absorbance extinction coefficient of 27 960 $M^{-1}.cm^{-1}$. The nanoparticles were diluted in the same solution and degassed. Reverse ITC experiments (nanoparticles in the cell) were performed at 25 °C, with a VP-ITC MicroCalorimeter from MicroCal Incorporated. Titration was performed with 10 µL injections of LecA solution (1.74 mM) in the 1.466 mL cell with nanoparticles solution ([glycoside] = 0.1 mM) every 300 s. Data were fitted with MicroCal PEAQ ITC analysis software according to standard procedures. Fitted data yielded the stoichiometry (n), the association constant (K_a) and the enthalpy of binding (ΔH). Other thermodynamic parameters (i.e., changes in free energy, ΔG, and

entropy, ΔS) were calculated from the equation $\Delta G = \Delta H - T\Delta S = RT.\ln K_a$, in which T is the absolute temperature and R = 8.314 $J.mol^{-1}.K^{-1}$. Two independent titrations were performed for each type of nanoparticles tested.

2.6. Biological evaluation

2.6.1. Cell Culture

Human endothelial umbilical vein cells (HUVEC) and murine macrophage monocytes (J774.A1) were maintained as recommended. HUVEC cells were grown in Dulbeccos's Modified Eagle Medium (DMEM) high glucose supplemented with 10 % fetal bovine serum (FBS), penicillin (100 $U.mL^{-1}$) and streptomycin (100 $U.mL^{-1}$). J774.A1 were grown in Roswell Park Memorial Institute medium (RPMI) 1640 supplemented with 10 % FBS, penicillin (100 $U.mL^{-1}$) and streptomycin (100 $U.mL^{-1}$). Cells were maintained in a humid atmosphere at 37 °C with 5 % CO_2.

2.6.2. Cytotoxicity Study

In vitro cytotoxicity of the nanoparticles and their degradation products was evaluated on the two cell lines using 3-[4,5-dimethylthiazol-2-yl]-3,5diphenyltetrazolium bromide (MTT) assay. Cells were seeded in 100 µL of growth medium (2×10^4 $cells.mL^{-1}$ for HUVEC, 1.5×10^4 $cells.mL^{-1}$ for J774.A1) in 96-well plates and incubated for 24 h. After appropriate dilutions in growth medium, 100 µL of nanoparticles or degradation products mixtures were added on the cells and incubated for 72 h. After incubation, 20 µL of MTT solution (5 $mg.mL^{-1}$ in PBS) was added to each well. The plates were incubated 1 h at 37 °C and the medium was removed. 200 µL of DMSO were then added to each well to dissolve the precipitates. Absorbance was measured at 570 nm using a plate reader (Metertech Σ 960, Fisher Bioblock, Illkirch, France). The percentage of surviving cells was calculated as the absorbance ratio of treated cells to untreated cells. All experiments, set up in sextuplicate, were performed at least 3 times with at least 2 different batches of nanoparticles or degradation products, to determine means and standard deviations (SD).

3. Results and Discussion

3.1. Synthesis of P(MTC-*co*-VE) copolymers

MTC was first copolymerized with BVE or TEGVE, two representative VE derivatives of opposite water solubility that were previously copolymerized with MDO.[22-23] Copolymerizations were performed in bulk at 70 °C for 8 h with $f_{MTC,0}$ = 0.8 and 3 mol % DEAB. ^{1}H NMR spectra of both copolymers (Figure 2a and Figure S1) confirmed the targeted structures, as shown by the proton signals *a–e* from MTC and those from the VE moiety (proton signals *g-j* in Figure 2a and *g-h* in Figure S1). Incorporation of VE units in the copolymer was also confirmed by proton signals ***a'*** and ***e'*** (Figure 2a and Figure S1). Both copolymers exhibited a composition similar to the initial comonomer feed ratio (F_{MTC} = 0.74 vs. $f_{MTC,0}$ = 0.8 for **P(MTC-*co*-BVE)** and F_{MTC} = 0.85 vs. $f_{MTC,0}$ = 0.80 for **P(MTC-*co*-TEGVA)**) and a quantitative ring-opening of MTC as evidenced by the absence of the acetal carbon signal in the δ = 100–110 ppm region on the ^{13}C NMR spectra (Figure S2-S3). It is well known that CKA monomers undergo H-transfer during polymerization, which can occur intramolecularly via 1,7-H shift (back-bitting) or intermolecularly (H-transfer). This has been shown experimentally[47-49] and theoretically.[50] The amount of branching is very dependent on monomer conversion[48] and experimental conditions,[49] and was also assumed to increase with ring size.[50] This amount can be determined by ^{1}H NMR by comparing the integration of the methyl end-group signal (0.9 ppm) in the case of MDO to the methylene signal in a-position to the ester moiety -C(O)O-CH_2- (4 ppm), whereas for MTC the branching methyl end-group is close to 1.2 ppm. Note that the CH_3 of the butyl ether group of BVE has also a triplet at 0.9 ppm. For P(MDO-*co*-BVE), the integration of the signal at 0.9 ppm was similar to the combination of the signals at 0.9 and 1.2 ppm of P(MTC-*co*-BVE), suggesting a similar branching ratio for MDO and MTC. The same trend was obtained for P(MTC-*co*-TEGVE), as $I_{1.2\ ppm}$ / $I_{4\ ppm}$ = 0.25 and $I_{0.9\ ppm}$ / $I_{4\ ppm}$ = 0.28 for P(MDO-*co*-TEGVE), thus confirming similar branching for the two CKAs. The **P(MTC-*co*-BVE)** copolymer was obtained with M_n = 10 800

g.mol^{-1} (*Đ* = 4.8), while the **P(MTC-*co*-TEGVE)** copolymer gave M_n = 7 300 g.mol^{-1} and *Đ* = 2.7 (Figure 2b and Figure S4). These results are in good agreement with the macromolecular characteristics of the MDO-based counterparts as **P(MDO-*co*-BVE)** gave M_n = 11 500 g.mol^{-1} (*Đ* = 3.6) and **P(MDO-*co*-TEGVE)** gave M_n = 8 000 g.mol^{-1} (*Đ* = 2.6) (Figure S5-S8, Table S1).

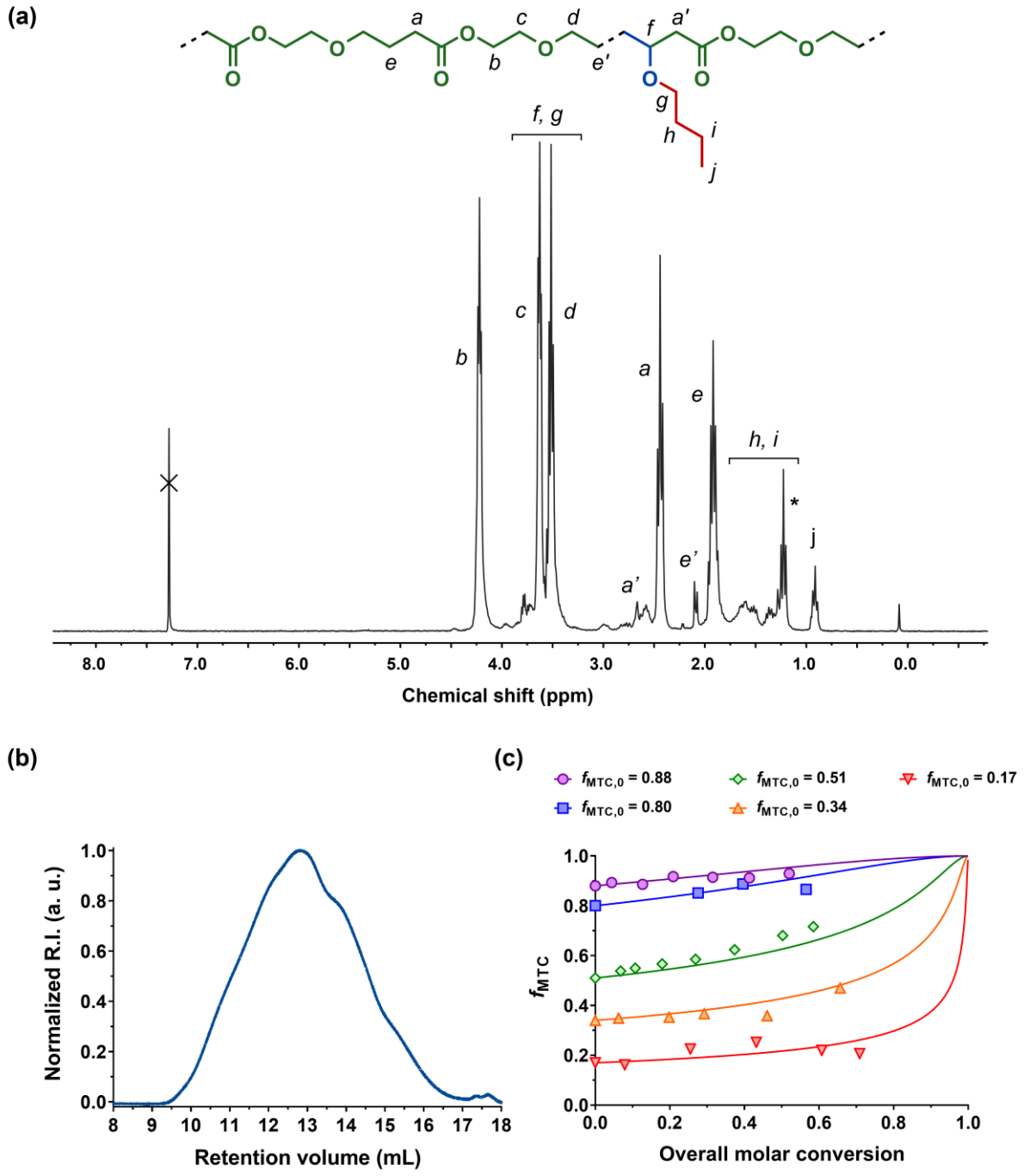

Figure 2. (a) ^{1}H NMR spectrum ($CDCl_3$) in the 0-8 ppm region of **P(MTC-*co*-BVE).** * = CH_3 from MTC backbiting. (b) SEC chromatogram ($CDCl_3$) of **P(MTC-*co*-BVE).** (c) Experimental (symbols) and theoretical (curves, with r_{MTC} = 0.36 ± 0.07 and r_{BVE} = 1.57 ± 0.17) evolution of the molar fraction of MTC in the feed vs. the overall molar conversion during bulk copolymerization of MTC and BVE (70 °C, 3 mol % DEAB).

To confirm a quasi-ideal free-radical copolymerization of MTC with VE monomers, similarly to that of MDO/VE copolymerization systems, we determined the reactivity ratios during the bulk copolymerization of MTC and BVE at 70 °C initiated by DEAB.[22] Using a non-linear least square (NLLS) fitting of the Skeist equation, we computed r_{MTC} = 0.36 ± 0.07 and r_{BVE} = 1.57 ± 0.17 (Figure 2c). These values are in the same order of magnitude as those obtained in the same conditions with MDO (r_{MDO} = 0.73 and r_{BVE} = 1.61).[22] This suggested a nearly ideal copolymerization between MTC and VE derivatives and therefore similar sequence distributions and copolymer compositions than with MDO. These results thus highlight a very good transposition from MDO to MTC during copolymerization with VE monomers.

To further illustrate this point, we synthesized a series of functional **P(MTC-*co*-VE)** copolymers based on their MDO counterparts: **P(MDO-*co*-CEVE)**, **P(MDO-*co*-IArVE)** and **P(MDO-*co*-GalVE)** (Table 1). While pendent chlorine atoms can be used for post-functionalization via nucleophilic substitution or substituted by azide groups to perform click chemistry,[22] IAr groups can serve as a handle to efficiently install thiosugar derivatives by the Buchwald−Hartwig−Migita cross-coupling method.[51] By transposing the polymerization procedures to MTC, the three MTC-based copolymers were successfully obtained (Figure S9-S14). MTC-based copolymers exhibited similar M_ns, dispersities and compositions than their MDO-based counterparts. These results therefore suggest that MTC can be copolymerized with a wide range of VE derivatives without significant differences from MDO.

Table 1. Macromolecular characteristics of the synthesized MTC-based functionalized copolymers.

Copolymer	$f_{MTC,0}$	F_{MTC}[a]	**MTC conv.[a] (%) / time (h)**	M_n **(g.mol^{-1})**	$Đ$

P(MTC-*co*-BVE)	0.80	0.85	94 / 8	10 800[b]	4.77[b]
P(MTC-*co*-TEGVE)	0.80	0.74	81 / 8	7 300[b]	2.71[b]
P(MTC-*co*-CEVE)	0.80	0.85	54 / 8	4 600[b]	2.47[b]
P(MTC-*co*-IArVE)	0.95	0.95	60 / 7	6 800[b]	4.90[b]
P(MTC-*co*-GalVE)	0.95	0.97	40 / 24	15 700[c]	1.55[c]

[a] Determined by ^{1}H NMR. [b] Determined by SEC in $CHCl_3$ (PMMA calibration). [c] Determined by SEC in DMSO with 0.1 mM LiBr (PMMA calibration).

3.2. Synthesis of P(MTC-*co*-MI) copolymers

We then studied the free-radical and RAFT copolymerizations of MTC with NEtMI as a maleimide derivative. FRP of NEtMI and MTC ($f_{MTC,0}$ = 0.5) was performed at 85 °C for 6 h in anhydrous toluene (0.5 M) and 2 mol % DEAB. The obtained **P(MTC-*co*-NEtMI)** copolymer gave M_n = 7 500 g.mol^{-1} ($Đ$ = 1.77) and F_{MTC} = 0.40 (Figure 3a,b). Conversion in NEtMI was nearly complete as suggested by the absence of the characteristic maleimide proton signal at 6.7 ppm on the ^{1}H NMR spectrum before purification (Figure 3a). ^{13}C NMR spectroscopy also evidenced the negligible ring-retaining propagation, given the near absence of signal corresponding to acetal carbons (δ = 100–110 ppm), as shown in Figure S15. The sequence distribution of the P(MTC-*co*-NEtMI) copolymer was then determined from the reactivity ratios using the NLLS method (Figure 3c), which gave r_{NEtMI} = 0.41 ± 0.07 and r_{MTC} = 0 ± 0.02. These values are very close to those reported for NEtMI/CKA,[19, 21] suggesting the formation of an alternating copolymer. This was confirmed by a 2D ^{1}H-^{13}C HMBC NMR experiment on P(MTC-*co*-NEtMI). The HMBC NMR spectrum exhibited a strong correlation between the CH_2 protons *e* at 1.8–2.2 ppm of MTC and one of the carbonyl carbons of NEtMI at 178.7 ppm (Figure S16). Moreover, no correlation between the CH_2 protons *e* and the carbonyl carbon of MTC was obtained, whereas the CH_2 protons *a* connected to the ester group of MTC and its carbonyl carbon gave a strong correlation, which further confirmed the alternating sequence.

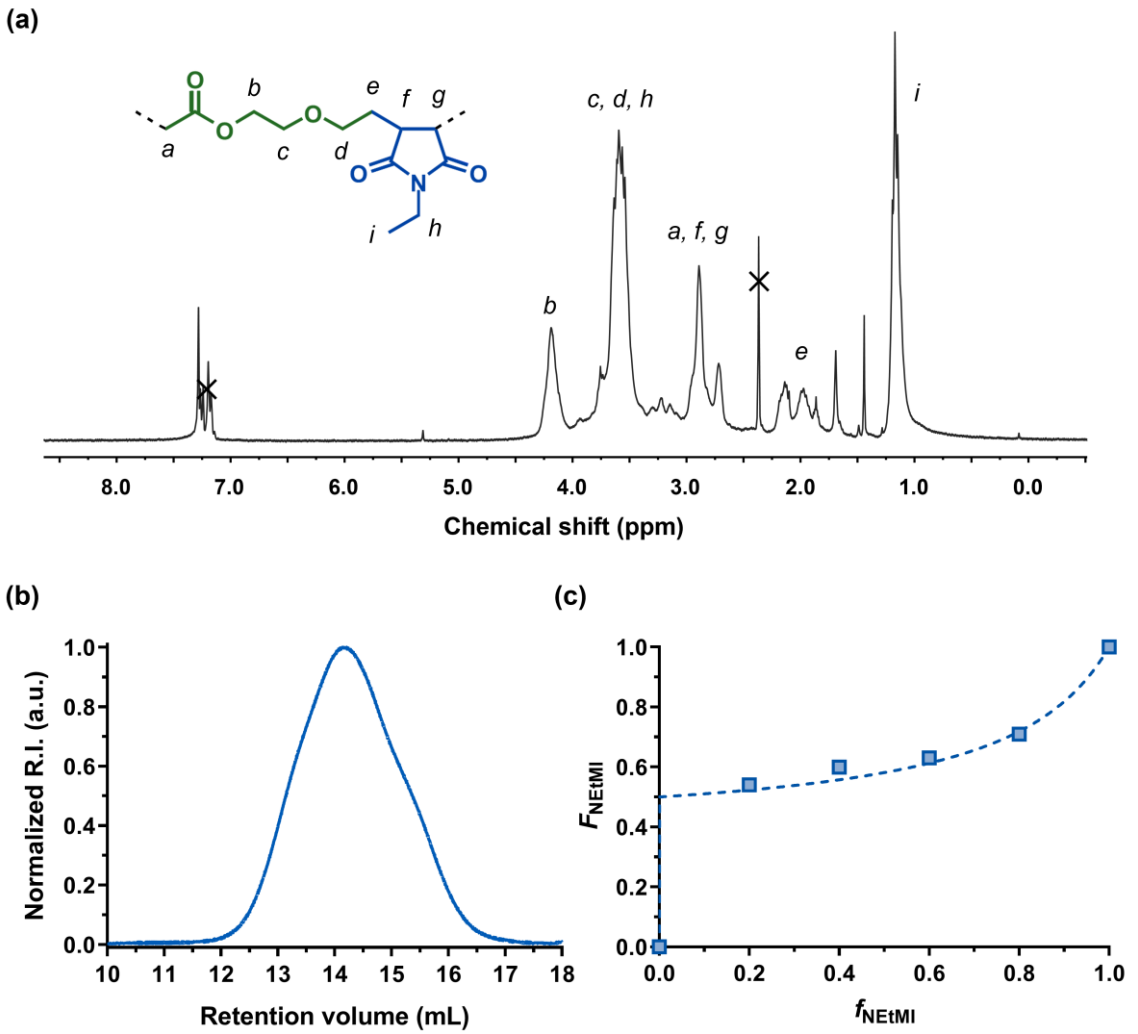

Figure 3. (a) ^{1}H NMR spectrum ($CDCl_3$) in the 0-8.0 ppm region of **P(MTC-*co*-NEtMI)** copolymer. (b) SEC chromatogram ($CHCl_3$) of **P(MTC-*co*-NEtMI)** copolymer. (c) Copolymer composition curve for the copolymerization of MTC and NEtMI in toluene ($[M]_0$ = 0.5 M, 85 °C, 2 mol % DEAB). Copolymerizations were stopped below 20% monomer conversion. The dashed line corresponds to the nonlinear least-squares fitting curve with r_{NEtMI} = 0.41 ± 0.07 and r_{MTC} = 0 ± 0.02.

To verify whether the transposition with MTC is also applicable to RDRP, RAFT copolymerization of MTC with NEtMI was studied using DDMAT as the chain transfer agent, which was previously used for the synthesis of P(BMDO-*co*-MI) copolymers (Figure 4a).[20] The copolymerization followed a pseudo-first-order kinetics up to ~8 h (NEtMI conv. = 40 %) (Figure 4b). It also exhibited a linear increase of the M_n with the NEtMI conversion, following the theoretical values, with dispersities ranging from 1.33 to 1.45, evidencing a reasonably good level of control (Figure 4c). Dispersities were nonetheless slightly higher than those

reported for the RAFT-mediated synthesis of P(BMDO-*co*-NEtMI) and P(MPDL-*co*-NEtMI) copolymers (*Đ* = 1.24–1.26).[19-20] This could be assigned to the influence of the structure of the CKA, even if the copolymerization parameters (e.g., monomer concentration, temperature, nature of the RAFT agent) may also be involved. Indeed, open MPDL and BMDO form a styryl- and benzyl-like propagating radical, respectively, whereas the radical ring-opening of MTC leads to a highly reactive primary radical, like MDO.

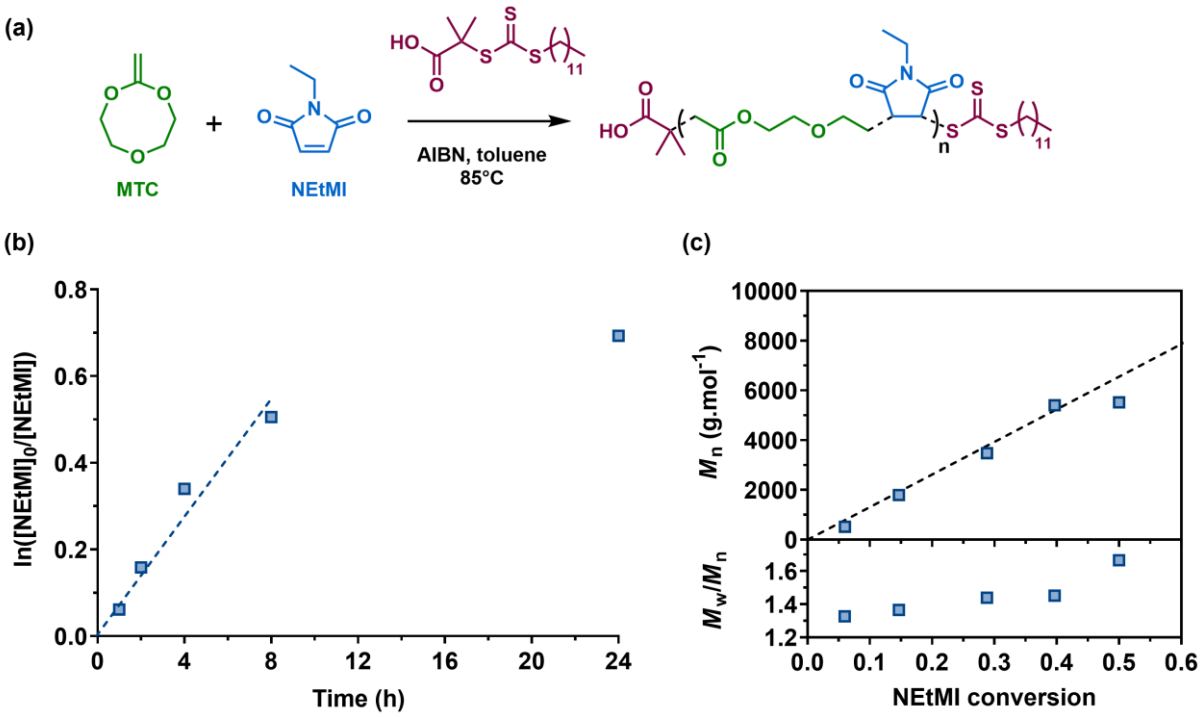

Figure 4. (a) RAFT copolymerization of MTC and NEtMI in toluene ($[M]_0$ = 0.5 M, 85 °C, $[MTC]_0$:$[NEtMI]_0$:$[DDMAT]_0$:$[AIBN]_0$ = 50:50:1:0.1). (b) Pseudo-first-order kinetic plot for the RAFT copolymerization of MTC and NEtMI. (c) Evolution of the number-average molecular weight (M_n) and dispersity ($Đ = M_w/M_n$) with NEtMI conversion.

3.3. Hydrolytic degradations in accelerated and physiological conditions

Given the more hydrophilic character of MTC, we then performed comparative hydrolytic degradations between **P(MDO-*co*-BVE)**, **P(MDO-*co*-TEGVE)** and **P(BMDO-*co*-NEtMI)** copolymers, and their MTC counterparts (Table S1 and Figures S17-S18), both under accelerated hydrolytic (0.05 wt % NaOH in MeOH:THF 1:1 v/v) and physiological (PBS, pH 7.4, 37°C) conditions (Figure 5 and Figures S19-S31). Note that the accelerated hydrolytic

degradation was performed in diluted conditions (about 10 times less concentrated) compared to the traditional conditions reported in the literature,[23] in order to better detect potential differences between the copolymers tested. By monitoring the decrease in M_w and M_n (even if M_w is more relevant since M_n is highly impacted by small chains) with time, all copolymers were fully degraded after ~30-45 min under accelerated hydrolytic conditions (Figure 5a–c and Figures S19–S25). Interestingly, while **P(BMDO-*co*-NEtMI)** and **P(MTC-*co*-NEtMI)** copolymers exhibited identical degradation kinetics (-90% in M_w after 15 min, Figure 5c), faster degradations were observed for **P(MTC-*co*-BVE)** and **P(MTC-*co*-TEGVE)** copolymers compared to their MDO counterparts (Figure 5a,b). The difference was even more pronounced with **P(MTC-*co*-BVE)**, leading to a decrease in M_w of 93 % for **P(MTC-co-BVE)** after 5 min vs. 53 % for **P(MDO-co-BVE)**. This shows that MTC units can efficiently promote water uptake/solvation of the ester groups despite the presence of strongly hydrophobic VE units.

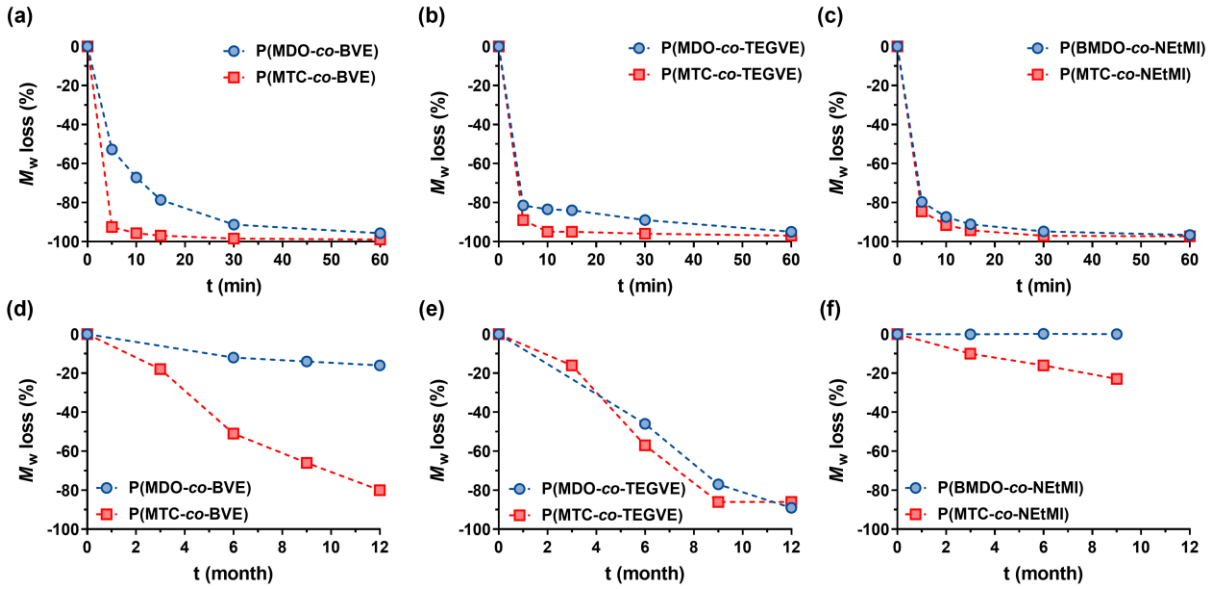

Figure 5. Evolution of the weight-average molar mass (M_w) during the hydrolytic degradation under accelerated conditions (0.05 wt % NaOH MeOH:THF 1:1 v/v) of: (a) **P(MDO-*co*-BVE)** and **P(MTC-*co*-BVE)** copolymers; (b) **P(MDO-*co*-TEGVE)** and **P(MTC-*co*-TEGVE)** copolymers and (c) **P(BMDO-*co*-NEtMI**) and **P(MTC-*co*-NEtMI)** copolymers. Evolution of M_w during the hydrolytic degradation under physiological conditions (PBS, pH 7.4, 37 °C) of: (d) **P(MDO-*co*-BVE)** and **P(MTC-*co*-BVE)**

copolymers; (e) **P(MDO-*co*-TEGVE)** and **P(MTC-*co*-TEGVE)** copolymers and (f) **P(BMDO-*co*-NEtMI)** and **P(MTC-*co*-NEtMI)** copolymers.

Hydrolytic degradations performed under physiological conditions were much slower; typically on a time scale of several months (Figure 5d–f, Figures S19 and Figures S26–S31). Interestingly, **P(MDO-*co*-TEGVE)** and **P(MTC-*co*-TEGVE)** copolymers exhibited rather similar degradation kinetics (~86 % decrease in M_w after 12 months, see Figure 5e), showing that MTC did not further promote cleavage of ester groups compared to MDO for such amphiphilic copolymers. However, a significant acceleration of the degradation was obtained for the hydrophobic **P(MTC-*co*-BVE)** copolymer (initially insoluble in PBS) compared to its MDO counterpart (Figure 5d). Indeed, **P(MDO-*co*-BVE)** gave a decrease in M_w of 16 % after 12 months, while **P(MTC-*co*-BVE)** was almost nearly degraded (85 % decrease in M_w). These results can be put in perspective with the degradation of traditional polyesters under identical experimental conditions.[24] While **P(MDO-*co*-BVE)** exhibited a degradation kinetics a bit slower than that of PCL, which can be explained by the structural similarity between PMDO and PCL, **P(MTC-*co*-BVE)** and **P(MDO-*co*-TEGVE)** copolymers degraded like PLA thanks to hydrophilic MTC and TEGVE moieties, respectively, which both promote water-uptake and solvation of ester groups. Hydrolytic degradation can now be accelerated by using either MTC as a hydrophilic CKA or a hydrophilic vinyl monomer.

Replacing BMDO by MTC also greatly improved the hydrolytic degradation under physiological conditions of hydrophobic NEtMI-based copolymers (Figure 5f). Indeed, while no degradation of **P(BMDO-*co*-NEtMI)** was observed after 9 months, **P(MTC-*co*-NEtMI)** gave a M_w decrease of ~23 % (Figure 5f), following a similar degradation kinetics than PCL.[24] This can be explained by the high hydrophobicity of BMDO, that prevents rapid water uptake and solvation of ester groups, conversely to MTC.

In conclusion, the use of MTC in place of MDO and BMDO allowed to: (i) shift from a PCL-like to a PLA-like hydrolytic degradation profile under physiological conditions for hydrophobic VE-based copolymers and (ii) induce a PCL-like degradation profile under

physiological conditions for the otherwise non-degradable NEtMI-based hydrophobic copolymers.

3.4. Application to degradable glycopolymer nanoparticles

In addition to promoting hydrolytic degradation, the hydrophilic properties of MTC were also investigated to improve the ligand-receptor molecular interactions of glycopolymer nanoparticles obtained by rROP. We recently developed degradable vinyl glyconanoparticles based on the formulation of **P(MDO-*co*-GalVE)** glycopolymers (Figure 6a).[44] They were obtained by copolymerization of MDO and protected GalVE, and subsequent deprotection. We observed that **P(MDO-*co*-GalVE)** glyconanoparticles exhibited limited interaction with LecA (K_d ~6 mM), a galactose-specific lectin, and suspected the establishment of non-specific hydrophobic interactions between LecA and the PCL-like backbone of the glycopolymers.

The **P(MTC-*co*-GalVE)** glycopolymer (Table 1, Figure 6a) was formulated into nanoparticles by surfactant-free nanoprecipitation. It produced narrowly dispersed nanoparticles of D_z = 134 nm (PSD = 0.02) and a ζ-potential of -20 mV (Figure 6b). The colloidal stability was assessed for at least 4 months at room temperature (Figure S32).

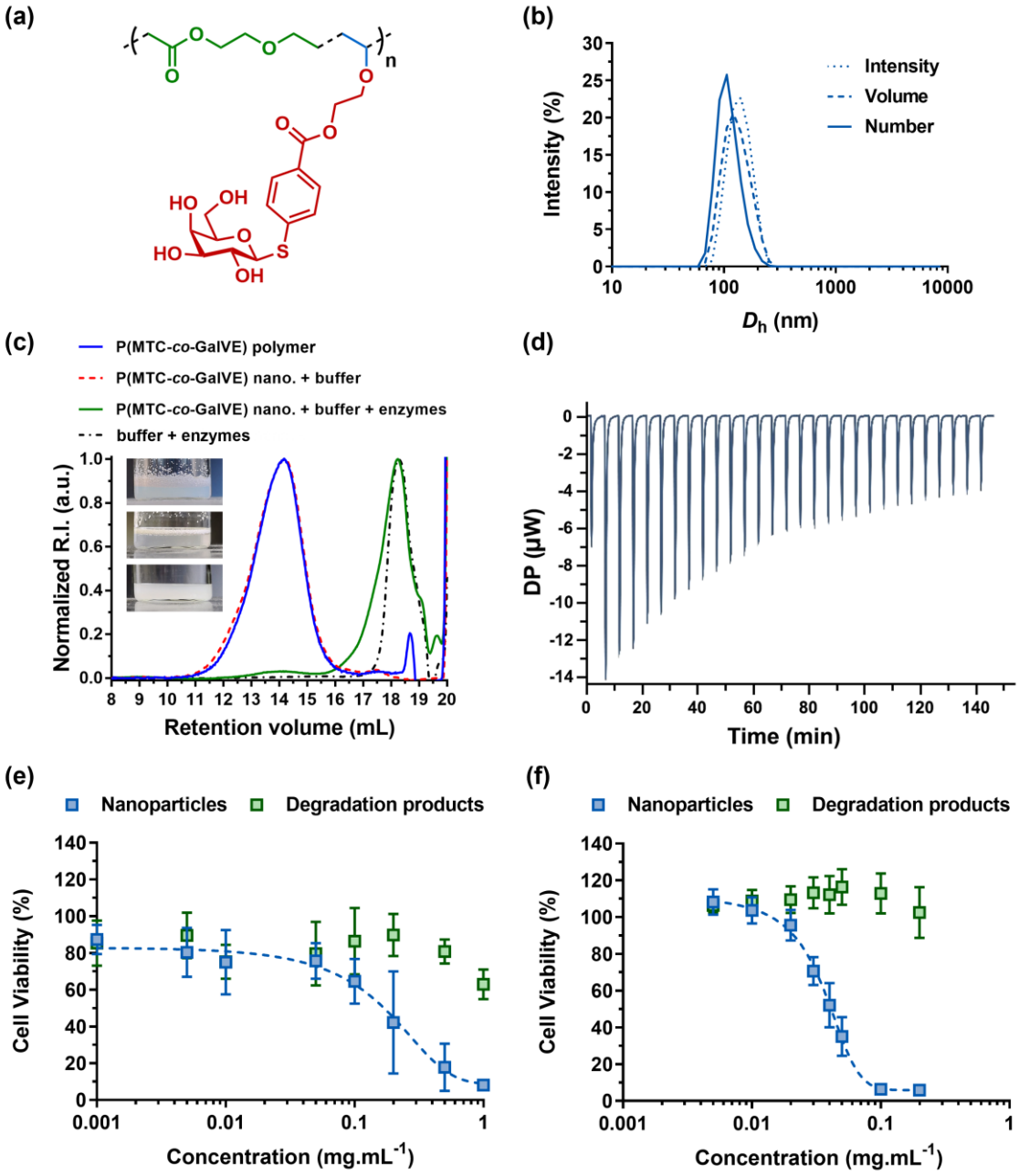

Figure 6. (a) Structure of the **P(MTC-*co*-GalVE)** glycopolymer. (b) Size distribution by intensity, volume and number of **P(MTC-*co*-GalVE)** glyconanoparticles. (c) SEC chromatogram ($CHCl_3$/TFA 0.1 vol %) of **P(MTC-*co*-GalVE)** glycopolymer and of **P(MTC-*co*-GalVE)** glyconanoparticles before and after enzymatic degradation (inserts: reaction mixture at t = 0 (top), t = 1 day (middle) with enzymes and t = 1 day without enzymes (bottom). (d) ITC thermogram obtained after injection of LecA (1.74 mM) onto **P(MTC-*co*-GalVE)** glyconanoparticles ([glycoside] = 0.1 mM). Cell viability (MTT assay) after incubation of: (e) HUVEC cells or (f) J774.A1 cells with increasing concentration of **P(MTC-*co*-GalVE)** glyconanoparticles and their degradation products. Results were expressed as percentages of absorption of treated cells ± SD.

Like **P(MDO-*co*-GalVE)** copolymer, **P(MTC-*co*-GalVE)** copolymer was enzymatically degraded in presence of Lipase B from *Candida antarctica*, an enzyme often used for the degradation of polyesters (Figure 6c).[52] After a 1-day incubation at 37 °C, the reaction mixture lost its blueish aspect (Tyndall effect) and became less cloudy, while an enzyme-free control stayed milky. SEC analyses showed a clear shift of the **P(MTC-*co*-GalVE)** chromatogram towards higher retention volumes, which evidenced a successful degradation into fragments of estimated M_w ~ 300 g.mol^{-1} (corresponding to a decrease in M_w of ~98 %). When the reaction was performed without Lipase B, no degradation occurred, which confirmed an enzyme-mediated degradation process.

We then studied the nanoparticle/LecA interactions by ITC (Figure 6d and Figure S33). The thermogram of **P(MTC-*co*-GalVE)** glyconanoparticles nearly exhibited a sigmoidal shape, leading to K_d ~5 µM (with an estimated 15% of accessible Gal units), which is 1200 times stronger affinity than with **P(MDO-*co*-GalVE)** glyconanoparticles.[44] The affinity is 10-fold higher than for the monosaccharide galactose, and in the same range as for the aryl-thiogalactoside present on the polymer.[53] This result is consistent with a specific carbohydrate-lectin interaction without cluster glycoside effect, i.e. without observing of a strong increase in affinity due to avidity.[54] These data thus suggest that a more hydrophilic copolymer backbone, through the use of MTC instead of MDO, led to a significant increase in the specific interaction between LecA and the corresponding glyconanoparticles, via a decrease in the non-specific hydrophobic interactions that have been hypothesized to mask the binding sites and/or galactose residues. Nevertheless, the absence of cluster glycoside effect was probably due to the polyester-like structure of **P(MTC-*co*-GalVE)** glycocopolymer which is composed of only ~5 mol % of glycosylated units.

Finally, we studied the cytotoxicity of **P(MTC-*co*-GalVE)** glyconanoparticles and their degradation products on HUVEC and J774.A1 cells, which are two representative healthy cell lines (Figure 6e,f). IC_{50} values were 0.04 mg.mL^{-1} on J774.A1 cells and 0.2 mg.mL^{-1} on HUVEC cells, which is similar to **P(MDO-*co*-GalVE)** glyconanoparticles under same conditions. Interestingly, degradation products did also not exhibit significant cytotoxicity on

the studied concentrations ranges, despite a slight decrease in cell viability at 1 $mg.mL^{-1}$ on HUVEC cells. These results showed that the replacement of MDO by MTC did not result in further decrease in cell viability.

4. Conclusion

In this study, we successfully reported the free-radical copolymerization of MTC with a library of VE derivatives to achieve degradable polyester-like copolymers. We also successfully copolymerized MTC with maleimides by either FRP and RAFT polymerization to obtain (well-defined) degradable alternating copolymers. For each copolymerization system, reactivity ratios confirmed the quasi-ideal statistical and alternating copolymerizations, respectively. Importantly, we showed that insertion of MTC units accelerated the hydrolytic degradation under physiological conditions of the corresponding hydrophobic copolymers compared to their counterparts obtained from traditional CKAs such as MDO, BMDO and MPDL.

Finally, MTC was used to prepare glycopolymers which were formulated into surfactant-free, enzymatically degradable glyconanoparticles. Interestingly, they exhibited interactions with LecA which were consistent with specific carbohydrate/lectin interactions, conversely to their MDO-counterparts which mainly exhibited non-specific hydrophobic interactions, likely due to the hydrophobicity of MDO. Preliminary cytotoxicity assays also demonstrated that MTC was as well tolerated as MDO by healthy cells, which is promising for biomedical applications.

Overall, these data established the beneficial effect of MTC, due to its greater hydrophilicity compared to the use of traditional hydrophobic CKAs, not only on the hydrolytic degradation rate of vinyl copolymers obtained by rROP, but also on the selectivity and intensity of ligand-receptor molecular interactions of gycopolymer nanoparticles with lectins.

Supporting Information

^{1}H, ^{13}C NMR and ^{1}H-^{13}C spectra of the copolymers, SEC of the copolymers before and during degradation, macromolecular characteristics of the copolymers used for degradation,

evolution of the molar masses of the copolymers with time during degradation, colloidal characteristics of the glyconanoparticles and ITC data.

Acknowledgments

We thank the ANR NanoCardioROP (ANR-15-CE08-0019) and the French Ministry of Research, respectively for the financial support of the Master 2 internship and the PhD thesis of TP. AI and EG acknowledge support from Glyco@Alps (ANR-15-IDEX-02) and Labex Arcane/CBH-EUR-GS (ANR-17-EURE-0003). Nathan Perrigault (IGPS, Univ Paris-Saclay), Didier Desmaële (IGPS, Univ Paris-Saclay) and Remi Franco (BioCIS, Univ Paris-Saclay) are acknowledged for technical assistance in 2D NMR experiments, Joseph Lumba is acknowledged for his help with the RAFT experiments and Stéphanie Denis (IGPS, Univ Paris-Saclay) is acknowledged for technical assistance in cell culture.

Table of Contents Graphic

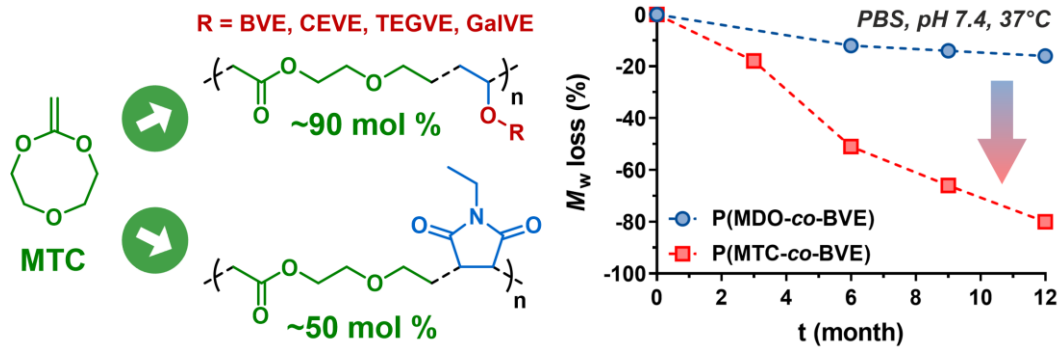

References

1. Hule, R. A.; Pochan, D. J., Polymer Nanocomposites for Biomedical Applications. *MRS Bull.* **2007,** *32* (4), 354-358.
2. Modjarrad, K.; Ebnesajjad, S., *Handbook of polymer applications in medicine and medical devices*. Elsevier: 2013.
3. Puoci, F.; Iemma, F.; Spizzirri, U. G.; Cirillo, G.; Curcio, M.; Picci, N., Polymer in agriculture: a review. *Am. J. Agric. Biol. Sci.* **2008,** *3* (1), 299-314.
4. Plastics-Europe Plastics - the Facts 2020. https://plasticseurope.org/knowledge-hub/plastics-the-facts-2020/ (accessed 06/01/2022).
5. Arutchelvi, J.; Sudhakar, M.; Arkatkar, A.; Doble, M.; Bhaduri, S.; Uppara, P. V., Biodegradation of polyethylene and polypropylene. *Indian J. Biotechnol.* **2008,** *7*, 9-22.
6. Sun, H.; Mei, L.; Song, C.; Cui, X.; Wang, P., The in vivo degradation, absorption and excretion of PCL-based implant. *Biomaterials* **2006,** *27* (9), 1735-1740.

7. Daghighi, S.; Sjollema, J.; van der Mei, H. C.; Busscher, H. J.; Rochford, E. T., Infection resistance of degradable versus non-degradable biomaterials: an assessment of the potential mechanisms. *Biomaterials* **2013,** *34* (33), 8013-8017.

8. Shastri, V. P., Non-degradable biocompatible polymers in medicine: past, present and future. *Curr. Pharm. Biotechnol.* **2003,** *4* (5), 331-337.

9. Vasir, J. K.; Reddy, M. K.; Labhasetwar, V. D., Nanosystems in drug targeting: opportunities and challenges. *Curr. Nanosci.* **2005,** *1* (1), 47-64.

10. Markovsky, E.; Baabur-Cohen, H.; Eldar-Boock, A.; Omer, L.; Tiram, G.; Ferber, S.; Ofek, P.; Polyak, D.; Scomparin, A.; Satchi-Fainaro, R., Administration, distribution, metabolism and elimination of polymer therapeutics. *J. Control. Release* **2012,** *161* (2), 446-460.

11. Barz, M.; Luxenhofer, R.; Zentel, R.; Vicent, M. J., Overcoming the PEG-addiction: well-defined alternatives to PEG, from structure–property relationships to better defined therapeutics. *Polym. Chem.* **2011,** *2* (9), 1900-1918.

12. Webster, R.; Elliott, V.; Park, B. K.; Walker, D.; Hankin, M.; Taupin, P., PEG and PEG conjugates toxicity: towards an understanding of the toxicity of PEG and its relevance to PEGylated biologicals. In *PEGylated Protein Drugs: Basic Science and Clinical Applications*, Veronese, F. M., Ed. Birkhäuser Basel: Basel, 2009; pp 127-146.

13. Dechy-Cabaret, O.; Martin-Vaca, B.; Bourissou, D., Controlled ring-opening polymerization of lactide and glycolide. *Chem. Rev.* **2004,** *104* (12), 6147-6176.

14. Delplace, V.; Nicolas, J., Degradable vinyl polymers for biomedical applications. *Nat. Chem.* **2015,** *7* (10), 771-784.

15. Pesenti, T.; Nicolas, J., 100th Anniversary of Macromolecular Science Viewpoint: Degradable Polymers from Radical Ring-Opening Polymerization: Latest Advances, New Directions, and Ongoing Challenges. *ACS Macro Lett.* **2020,** *9* (12), 1812-1835.

16. Tardy, A.; Nicolas, J.; Gigmes, D.; Lefay, C.; Guillaneuf, Y., Radical ring-opening polymerization: Scope, limitations, and application to (bio) degradable materials. *Chem. Rev.* **2017,** *117* (3), 1319-1406.

17. Agarwal, S., Chemistry, chances and limitations of the radical ring-opening polymerization of cyclic ketene acetals for the synthesis of degradable polyesters. *Polym. Chem.* **2010,** *1*, 953-964.

18. Jackson, A. W., Reversible-deactivation radical polymerization of cyclic ketene acetals. *Polym. Chem.* **2020,** *11* (21), 3525-3545.

19. Hill, M. R.; Guégain, E.; Tran, J.; Figg, C. A.; Turner, A. C.; Nicolas, J.; Sumerlin, B. S., Radical ring-opening copolymerization of cyclic ketene acetals and maleimides affords homogeneous incorporation of degradable units. *ACS Macro Lett.* **2017,** *6* (10), 1071-1077.

20. Hill, M. R.; Kubo, T.; Goodrich, S. L.; Figg, C. A.; Sumerlin, B. S., Alternating radical ring-opening polymerization of cyclic ketene acetals: access to tunable and functional polyester copolymers. *Macromolecules* **2018,** *51* (14), 5079-5084.

21. Shi, Y.; Agarwal, S., Thermally stable optically transparent copolymers of 2-methylene-1, 3-dioxepane and N-phenyl maleimide with degradable ester linkages. *e-Polymers* **2015,** *15* (4), 217-226.

22. Tardy, A.; Honoré, J. C.; Tran, J.; Siri, D.; Delplace, V.; Bataille, I.; Letourneur, D.; Perrier, J.; Nicoletti, C.; Maresca, M., Radical copolymerization of vinyl ethers and cyclic ketene acetals as a versatile platform to design functional polyesters. *Angew. Chem. Int. Ed.* **2017,** *129* (52), 16742-16747.

23. Tran, J.; Pesenti, T.; Cressonnier, J.; Lefay, C.; Gigmes, D.; Guillaneuf, Y.; Nicolas, J., Degradable copolymer nanoparticles from radical ring-opening copolymerization between cyclic ketene acetals and vinyl ethers. *Biomacromolecules* **2018,** *20* (1), 305-317.

24. Guégain, E.; Michel, J.-P.; Boissenot, T.; Nicolas, J., Tunable degradation of copolymers prepared by nitroxide-mediated radical ring-opening polymerization and point-by-point comparison with traditional polyesters. *Macromolecules* **2018,** *51* (3), 724-736.

25. Bossion, A.; Zhu, C.; Guerassimoff, L.; Mougin, J.; Nicolas, J., Vinyl copolymers with faster hydrolytic degradation than aliphatic polyesters and tunable upper critical solution temperatures. *Nature Commun.* **2022,** *13* (1), 2873.

26. Folini, J.; Huang, C.-H.; Anderson, J. C.; Meier, W. P.; Gaitzsch, J., Novel monomers in radical ring-opening polymerisation for biodegradable and pH responsive nanoparticles. *Polym. Chem.* **2019,** *10* (39), 5285-5288.

27. Yako, N.; Endo, T., Syntheses and radical ring-opening polymerization of cyclic keten acetals. *Polym. Prepr. Jpn.* **1985,** *34*, 154.

28. Hiraguri, Y.; Tokiwa, Y., Syntheses of biodegradable functional polymers by radical ring-opening polymerization of 2-methylene-1, 3, 6-trioxocane. *J. Polym. Environ.* **2010,** *18* (2), 116-121.

29. Folini, J.; Murad, W.; Mehner, F.; Meier, W.; Gaitzsch, J., Updating radical ring-opening polymerisation of cyclic ketene acetals from synthesis to degradation. *Eur. Polym. J.* **2020,** *134*, 109851.

30. Hiracuri, Y.; Tokiwa, Y., Synthesis of copolymers composed of 2-methylene-1, 3, 6-trioxocane and vinyl monomers and their enzymatic degradation. *J. Polym. Sci., Part A: Polym. Chem.* **1993,** *31* (12), 3159-3163.

31. Hiraguri, Y.; Tokiwa, Y., Synthesis of photodegradable polymers having biodegradability and their biodegradations and photolysis. *Macromolecules* **1997,** *30* (12), 3691-3693.

32. Hiraguri, Y.; Tokiwa, Y., Synthesis of a novel water-soluble copolymer composed of 2-methylene-1, 3, 6-trioxocane and N-vinyl 2-pyrrolidone and its enzymatic degradation. *Clean Products and Processes* **2001,** *3* (3), 303-306.

33. Hiraguri, Y.; Tokiwa, Y., Synthesis of thermosensitive polymers having enzymatic degradability. *Clean Technol. Environ. Policy* **2002,** *4* (2), 122-124.

34. Hiraguri, Y.; Katase, K.; Tokiwa, Y., Synthesis of Biodegradable Detergent Builder by Alternating Copolymerization of 2-Methylene-1, 3, 6-trioxocane and Maleic Anhydride. *J. Macromol. Sci. - Pure Appl. Chem.* **2007,** *44* (8), 893-897.

35. Hiraguri, Y.; Tokiwa, Y., Synthesis of a new gel with enzymatic degradability. *J. Mater. Sci. Lett.* **2002,** *21* (23), 1875-1876.

36. Hiraguri, Y.; Katase, K.; Tokiwa, Y., Synthesis of Biodegradable Hydrogel by Radical Ring-Opening Polymerization of 2-Methylene-1, 3, 6-Trioxocane. *J. Macromol. Sci. - Pure Appl. Chem.* **2006,** *43* (7), 1021-1027.

37. Hiraguri, Y.; Katase, K.; Tokiwa, Y., Biodegradability of Poly (ester-ether) and Poly (ester) Obtained from a Radical Ring-Opening Polymerization of Cyclic Ketene Acetals. *J. Macromol. Sci. - Pure Appl. Chem.* **2005,** *42* (7), 901-907.

38. Undin, J.; Plikk, P.; Finne-Wistrand, A.; Albertsson, A. C., Synthesis of amorphous aliphatic polyester-ether homo-and copolymers by radical polymerization of ketene acetals. *J. Polym. Sci., Part A: Polym. Chem.* **2010,** *48* (22), 4965-4973.

39. Zeng, T.; You, W.; Chen, G.; Nie, X.; Zhang, Z.; Xia, L.; Hong, C.; Chen, C.; You, Y., Degradable PE-Based Copolymer with Controlled Ester Structure Incorporation by Cobalt-Mediated Radical Copolymerization under Mild Condition. *iScience* **2020,** *23* (3), 100904.

40. Zeng, T.-Y.; Xia, L.; Zhang, Z.; Hong, C.-Y.; You, Y.-Z., Dithiocarbamate-mediated controlled copolymerization of ethylene with cyclic ketene acetals towards polyethylene-based degradable copolymers. *Polym. Chem.* **2021,** *12* (2), 165-171.

41. Du, Y.; Du, Y.; Lazzari, S.; Reimers, T.; Konradi, R.; Holcombe, T. W.; Coughlin, E. B., Mechanistic investigation of cyclic ketene acetal radical ring-opening homo- and co-polymerization and preparation of PEO graft copolymers with tunable composition. *Polym. Chem.* **2022,** *13* (41), 5829-5840.

42. Cioci, G.; Mitchell, E. P.; Gautier, C.; Wimmerová, M.; Sudakevitz, D.; Pérez, S.; Gilboa-Garber, N.; Imberty, A., Structural basis of calcium and galactose recognition by the lectin PA-IL of Pseudomonas aeruginosa. *FEBS Lett.* **2003,** *555* (2), 297-301.

43. Gilboa-Garber, N., Pseudomonas aeruginosa lectins. In *Methods Enzymol.*, Elsevier: 1982; Vol. 83, pp 378-385.

44. Pesenti, T.; Domingo-Lopez, D.; Gillon, E.; Ibrahim, N.; Messaoudi, S.; Imberty, A.; Nicolas, J., Degradable Glycopolyester-like Nanoparticles by Radical Ring-Opening Polymerization. *Biomacromolecules* **2022,** *23* (9), 4015-4028.

45. Blanchard, B.; Nurisso, A.; Hollville, E.; Tetaud, C.; Wiels, J.; Pokorná, M.; Wimmerová, M.; Varrot, A.; Imberty, A., Structural basis of the preferential binding for globo-series glycosphingolipids displayed by Pseudomonas aeruginosa lectin I. *J. Mol. Biol.* **2008,** *383* (4), 837-853.

46. Tran, J.; Guégain, E.; Ibrahim, N.; Harrisson, S.; Nicolas, J., Efficient synthesis of 2-methylene-4-phenyl-1, 3-dioxolane, a cyclic ketene acetal for controlling the NMP of methyl methacrylate and conferring tunable degradability. *Polym. Chem.* **2016,** *7* (26), 4427-4435.

47. Jin, S.; Gonsalves, K. E., A Study of the Mechanism of the Free-Radical Ring-Opening Polymerization of 2-Methylene-1,3-dioxepane. *Macromolecules* **1997,** *30* (10), 3104-3106.

48. Tardy, A.; Honoré, J.-C.; Siri, D.; Nicolas, J.; Gigmes, D.; Lefay, C.; Guillaneuf, Y., A comprehensive kinetic study of the conventional free-radical polymerization of seven-membered cyclic ketene acetals. *Polym. Chem.* **2017,** *8* (34), 5139-5147.

49. Mehner, F.; Geisler, M.; Arnhold, K.; Komber, H.; Gaitzsch, J., Structure–Property Relationships in Polyesters from UV-Initiated Radical Ring-Opening Polymerization of 2-Methylene-1,3-dioxepane (MDO). *ACS Appl. Polym. Mater.* **2022,** *4* (10), 7891-7902.

50. Reddy Mothe, S.; Tan, J. S. J.; Chennamaneni, L. R.; Aidil, F.; Su, Y.; Kang, H. C.; Lim, F. C. H.; Thoniyot, P., A systematic investigation of the ring size effects on the free radical ring-opening polymerization (rROP) of cyclic ketene acetal (CKA) using both experimental and theoretical approach. *J. Polym. Sci.* **2020,** *58* (12), 1728-1738.

51. Pesenti, T.; Domingo-Lopez, D.; Gillon, E.; Ibrahim, N.; Imberty, A.; Messaoudi, S.; Nicolas, J., Degradable Glycopolyester-like Nanoparticles by Radical Ring- Opening Polymerization. *Biomacromolecules* **2022,** *23* (9), 4015-4028.

52. Kundys, A.; Białecka-Florjańczyk, E.; Fabiszewska, A.; Małajowicz, J., Candida antarctica lipase B as catalyst for cyclic esters synthesis, their polymerization and degradation of aliphatic polyesters. *J. Polym. Environ.* **2018,** *26* (1), 396-407.

53. Rodrigue, J.; Ganne, G.; Blanchard, B.; Saucier, C.; Giguère, D.; Shiao, T. C.; Varrot, A.; Imberty, A.; Roy, R., Aromatic thioglycoside inhibitors against the virulence factor LecA from Pseudomonas aeruginosa. *Org. Biomol. Chem.* **2013,** *11* (40), 6906-6918.

54. Lee, R. T.; Lee, Y. C., Affinity enhancement by multivalent lectin–carbohydrate interaction. *Glycoconj. J.* **2000,** *17* (7), 543-551.